# Supplementary Information

**TIAF1 self-aggregation in peritumor capsule formation, spontaneous activation of SMAD-responsive promoter in p53-deficient environment, and cell death**

Jean-Yun Chang, Ming-Fu Chiang, Sing-Ru Lin, Ming-Hui Lee, Huang He, Pei-Yi Chou, Szu-Jung Chen, Yu-An Chen, Li-Yi Yang, Feng-Jie Lai, Chih-Chin Hsieh, Ting-Hui Hsieh, Hamm-Ming Sheu, Chun-I Sze, Nan-Shan Chang

## References

1. Chang NS, Mattison J, Cao H, Pratt N, Zhao Y, Lee C. Cloning and characterization of a novel transforming growth factor-β1-induced TIAF1 protein that inhibits tumor necrosis factor cytotoxicity. *Biochem Biophys Res Commun* 1998; **253**: 743-749.

2. Chen ST, Chuang JI, Cheng CL, Hsu LJ, Chang NS. Light-induced retinal damage involves tyrosine 33 phosphorylation, mitochondrial and nuclear translocation of WW domain-containing oxidoreductase *in vivo*. *Neuroscience* 2005; **130**: 397-407.

**Figure S1. Testing the validity of TIAF1 antibody by a blocking peptide**.

**(a)** Human skin melanoma tissue sections were stained with homemade TIAF1(R48-2)[1] and commercial TIAF1(Abcam) antibodies, in the presence or absence of a blocking R48-2 peptide (20 μM).[2] Nuclei were stained with DAPI. The peptide blocked the immunoreactivity of both antibodies. **(b)** Human neurofibromatosis NF1 tissue sections were stained with TIAF1(R48-2) antibody with or without using the blocking peptide. After taking pictures and stripping off, the slides were stained with the same antibody for color development (or IHC; left column). **(c)** The peptide blocked the immunoreactivity of TIAF1(R48-2), but not TIAF1(R48-1), antibody in human meningioma tissues. Scale bars for all images, 50 μm (200x magnification). Nuclei were stained with DAPI.

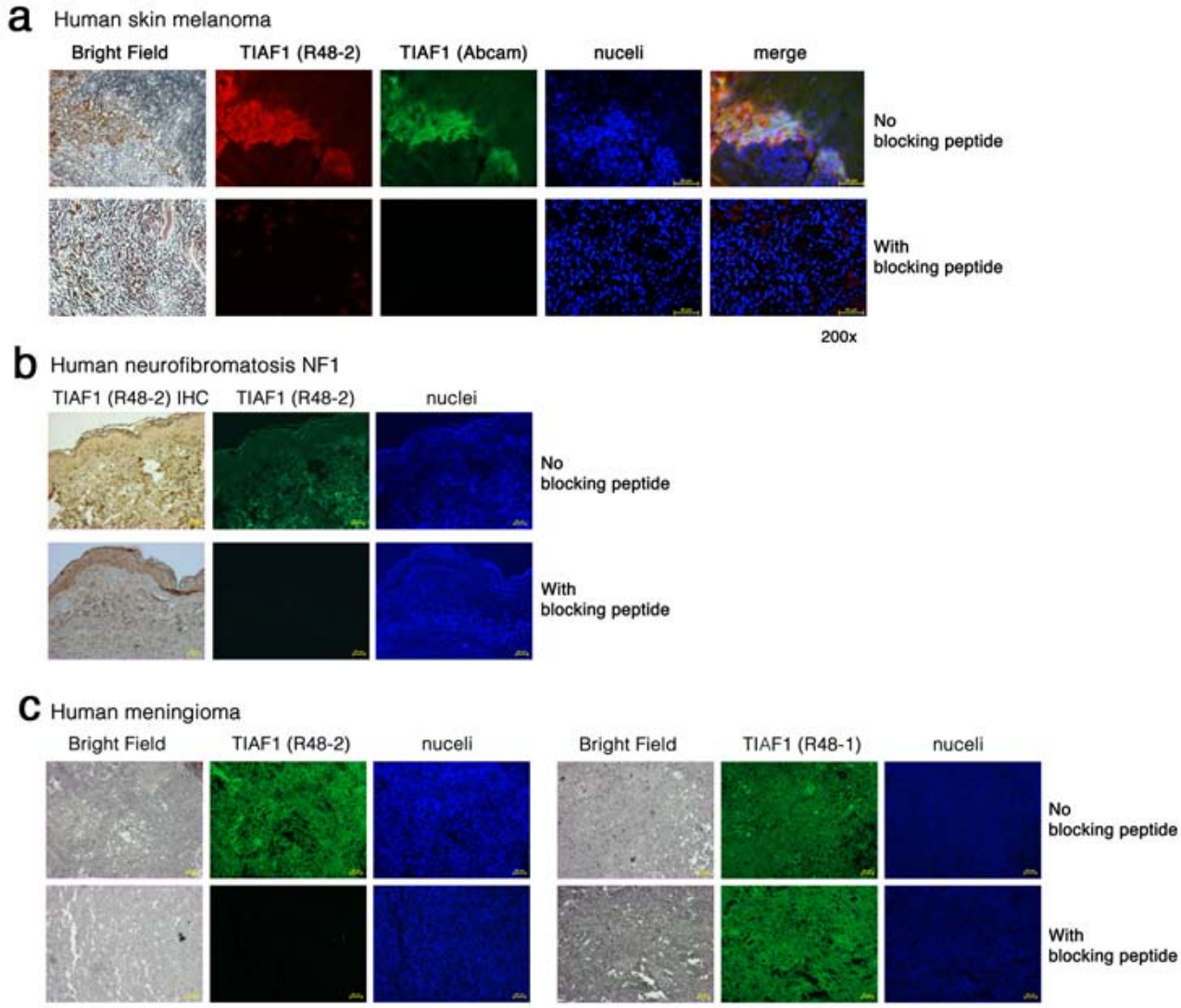


***Fig. S1***

**Figure S2. Downregulation of TIAF1 in breast cancer**.

(**a,b**) TIAF1 expression is shown in normal mammary gland cells, as determined using anti-TIAF1(R48-2) antibody by IHC. (**c-e**) TIAF1 expression is reduced in breast cancer tissue sections. (**f**) TIAF1 expression is shown in breast fibroadenoma. (**g,h,i**) Negative controls are the R48-2 peptide-blocked IHC staining of normal breast (**g**) and breast cancer (**h,i**). All scale bars are 100 μm, except in 50 μm for **g**,**i**.

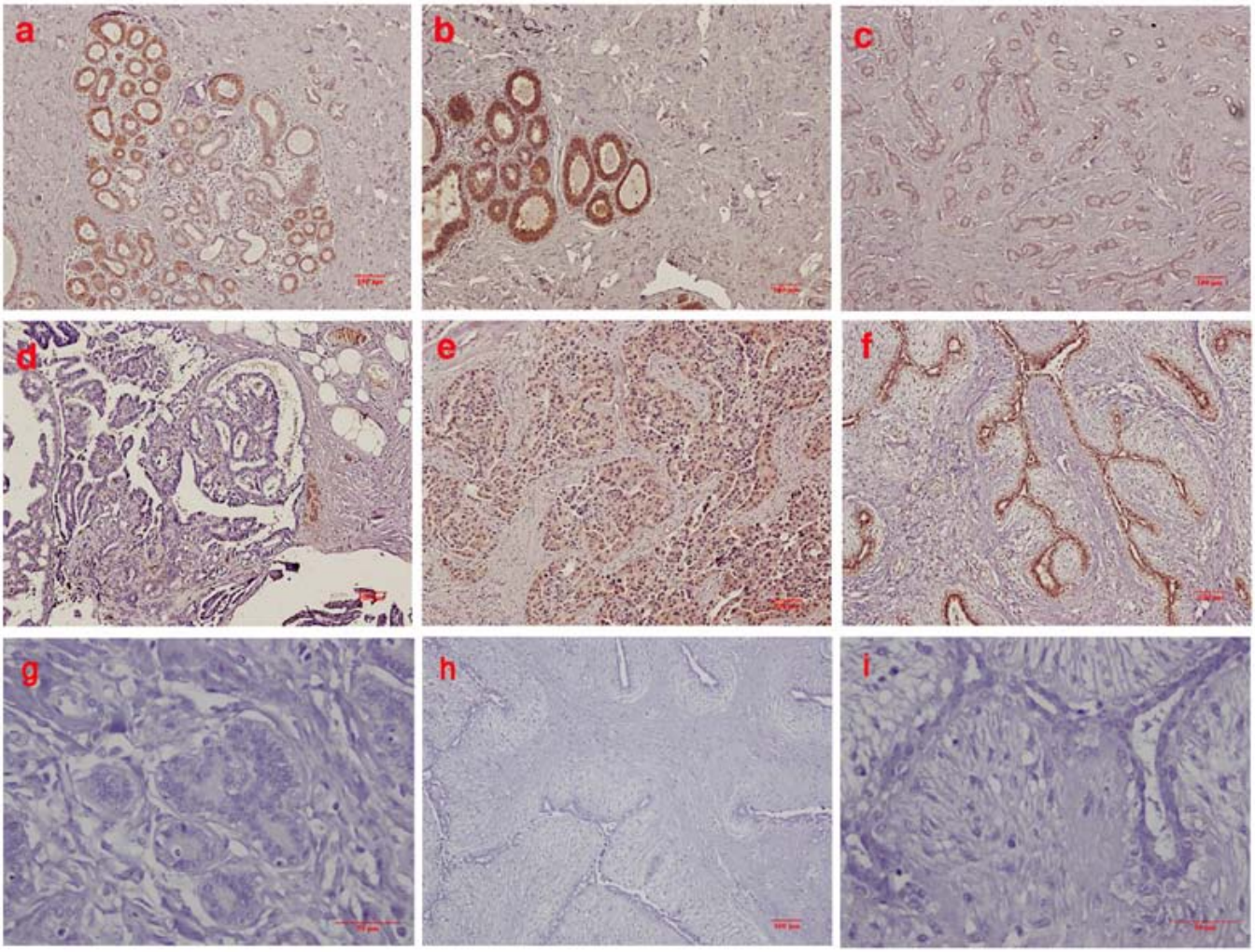

**Figure S3. Upregulation of TIAF1 and Smad4 in prostate cancer**.

**(a)** Compared to normal prostate, TIAF1 levels are increased by 50-120% in prostate cancer. Nuclei were stained with DAPI. Representative tissue sections were from staining 5 normal controls and 5 prostate cancer tissue sections. **(b)** TIAF1 co-localizes with Smad4 in the prostatic concretions in the lumens of prostatic glandular ducts. Both proteins are significantly upregulated in the non-metastatic prostate cancer. **(c)** Colocalization of TIAF1 and Smad4 is shown in the prostate gland cells. The "non-immune serum" control is shown in Figure 1c, and blocking peptide controls in Figure S4.

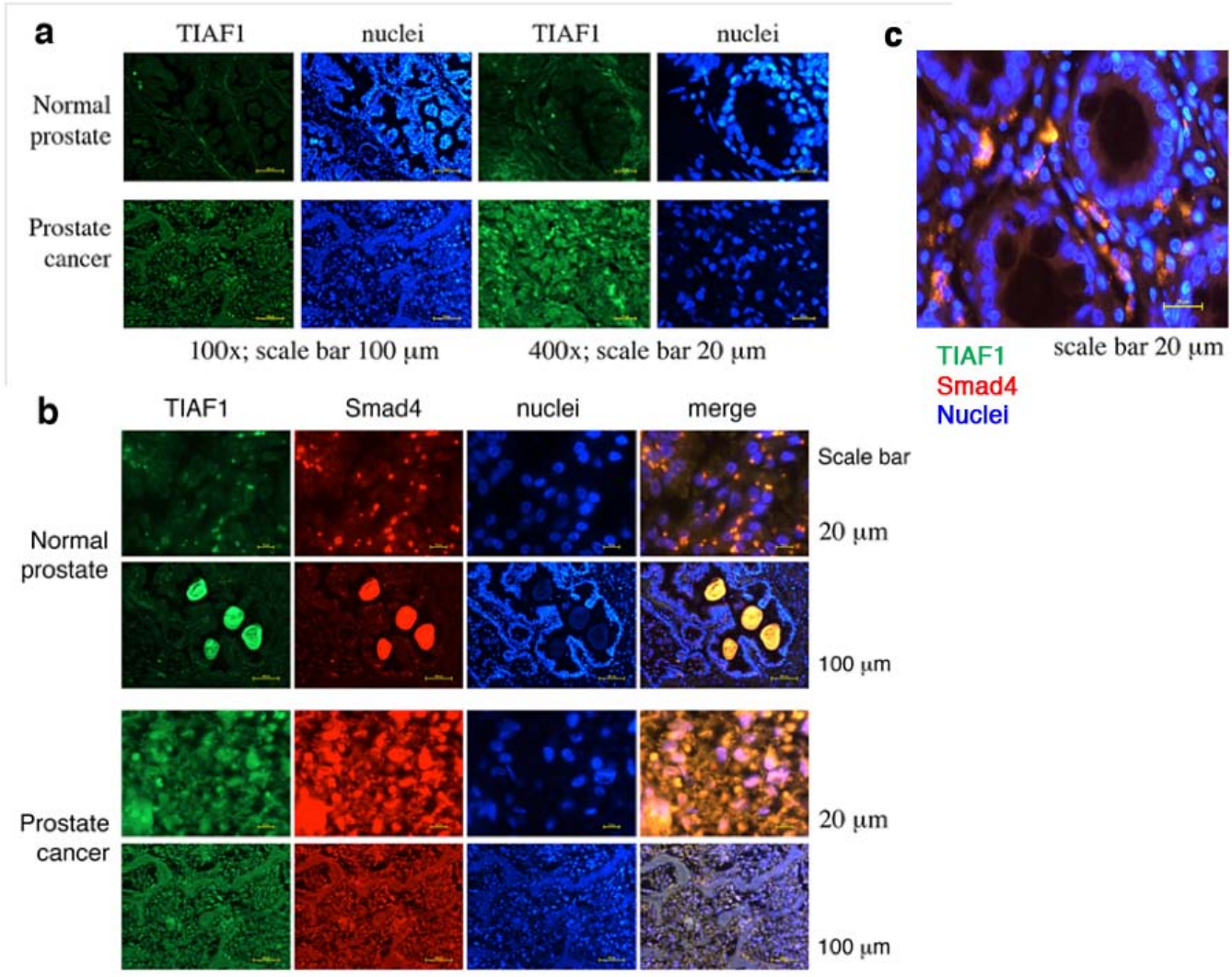


***Fig. S3***

**Figure S4. IHC staining of TIAF1 in the prostate tissues**.

In parallel with the above observations, TIAF1 has a higher level of expression in cancer, compared with the normal controls. Representative data is from 6 controls and 6 prostate cancers. Scale bar, 100 μm at left column (200x magnification), and 50 μm at right column (400x magnification). In negative controls, the R48-2 peptide was used to block the immunostaining.

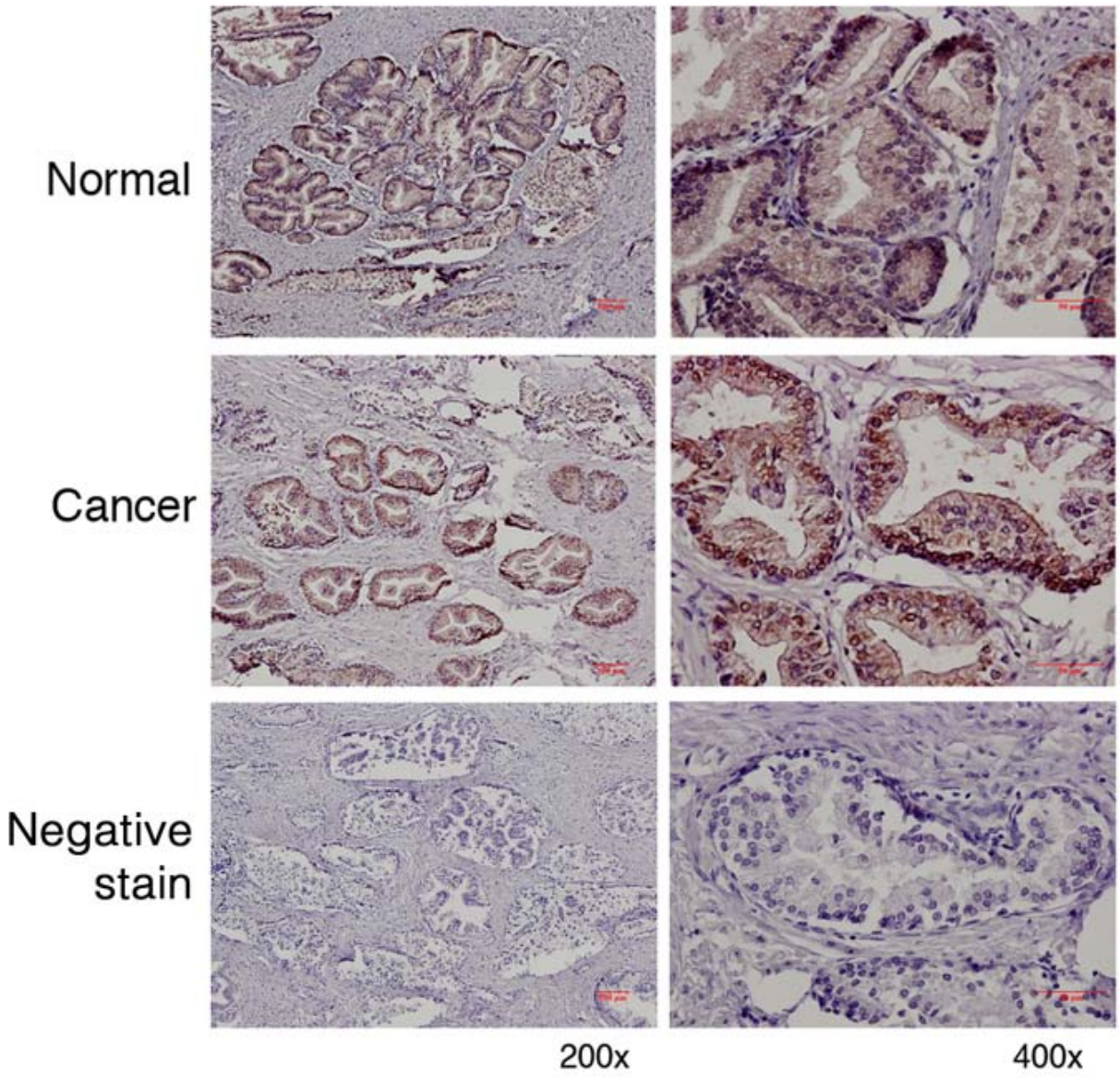


***Fig. S4***

**Figure S5. TIAF1 is significantly downregulated in the metastatic prostate cancer**.

By fluorescent immunostaining, TIAF1 and Smad4 expression are significantly downregulated in metastatic prostate cancer, compared to the non-malignant cancerous stages. The "non-immune serum" control is shown in Figure 1c, and blocking peptide controls in Figure S4.

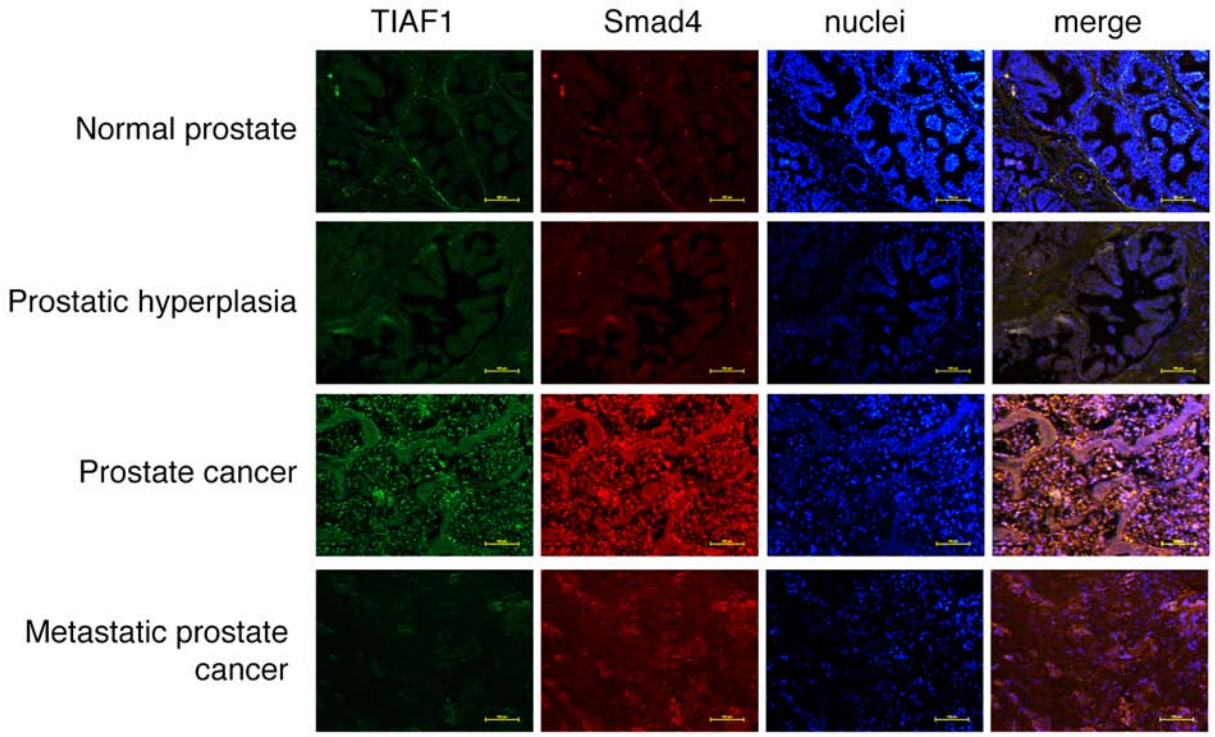


***Fig. S5***

**Figure S6. Upregulation of TIAF1 in the colon cancer tissues**.

TIAF1 (green) is significantly upregulated in colon cancer cells, as compared to age-matched controls. Also, the levels of Smad4 (red) are significantly increased in the colon cancer group compared with the normal controls. The number on top of each bar is the times for measuring a fixed square area in tissue sections from 5 samples or patients. Statistical analysis: normal versus cancer, Student's *t* test. In negative controls, fluorescent secondary antibodies were used only.

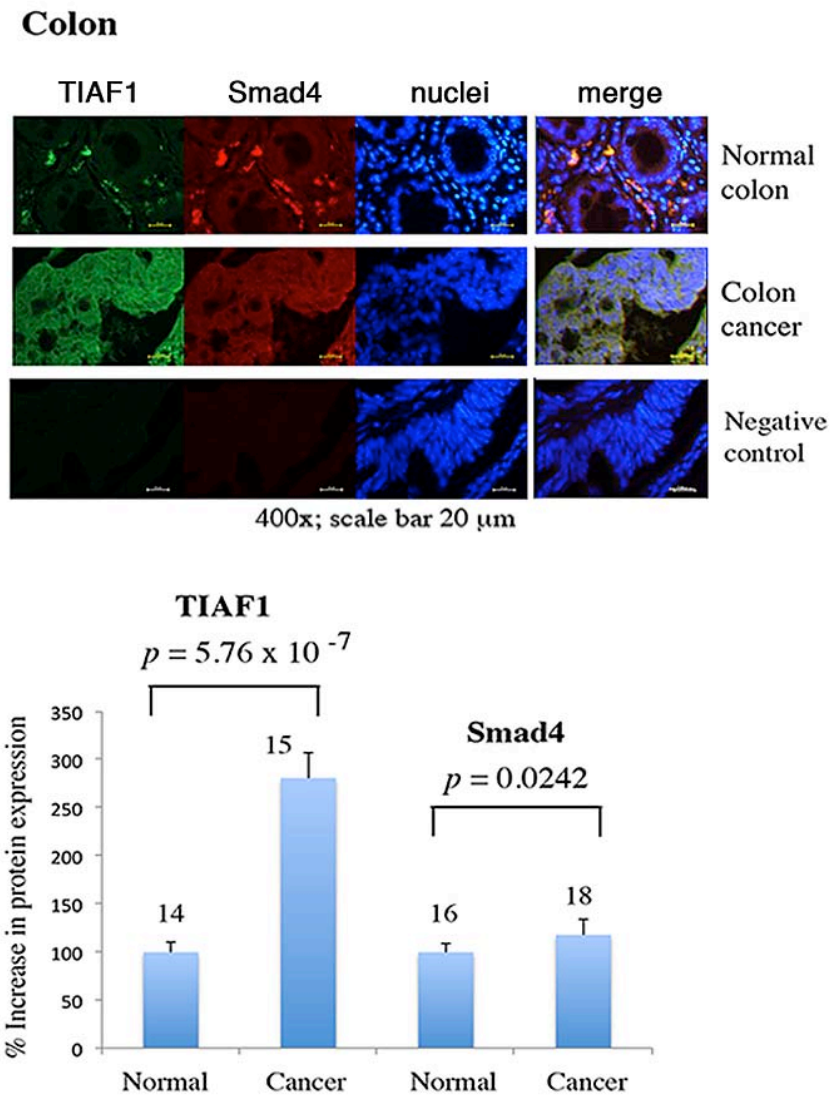


***Fig. S6***

**Figure S7. TIAF1 aggregates in the metastatic cancer in the brain**.

**(a)** A solid lung tumor in the brain of a patient was removed from surgery. By fluorescent immunostaining, TIAF1 aggregates are shown in the interface between the tumor (the area clouded with nuclei at the top right) and the brain. Degenerating neural cells were stained with Fluoro-Jade C Red. Nuclei were stained with DAPI. Scale bar, 20 mm; 400x magnification. Merge, overlay images for TIAF1, Fluoro-Jade C, and DAPI. **(b)** Similarly, presence of TIAF1 and Aβ aggregates is shown in another patient with a metastatic lung cancer in the brain. Note that TIAF1 does not perfectly colocalize with the Aβ aggregates. Scale bar, 20 mm; 400x magnification. **(c,d)** Presence of TIAF1 and Aβ aggregates is shown in the metastatic nasopharngeal carcinoma (NPC) in the brain (see merged picture in the left). TIAF1, green; Aβ, red; nuclei, blue. Scale bar, 20 mm; 400x magnification. Phase or bright field, pictures at the right column. (**e**) In negative controls, R48-2 peptide was used to block the immunostaining. Merge: TIAF1(Abcam), TIAF1(R48-2) and DAPI. Scale bar, 20 mm; 400x magnification.

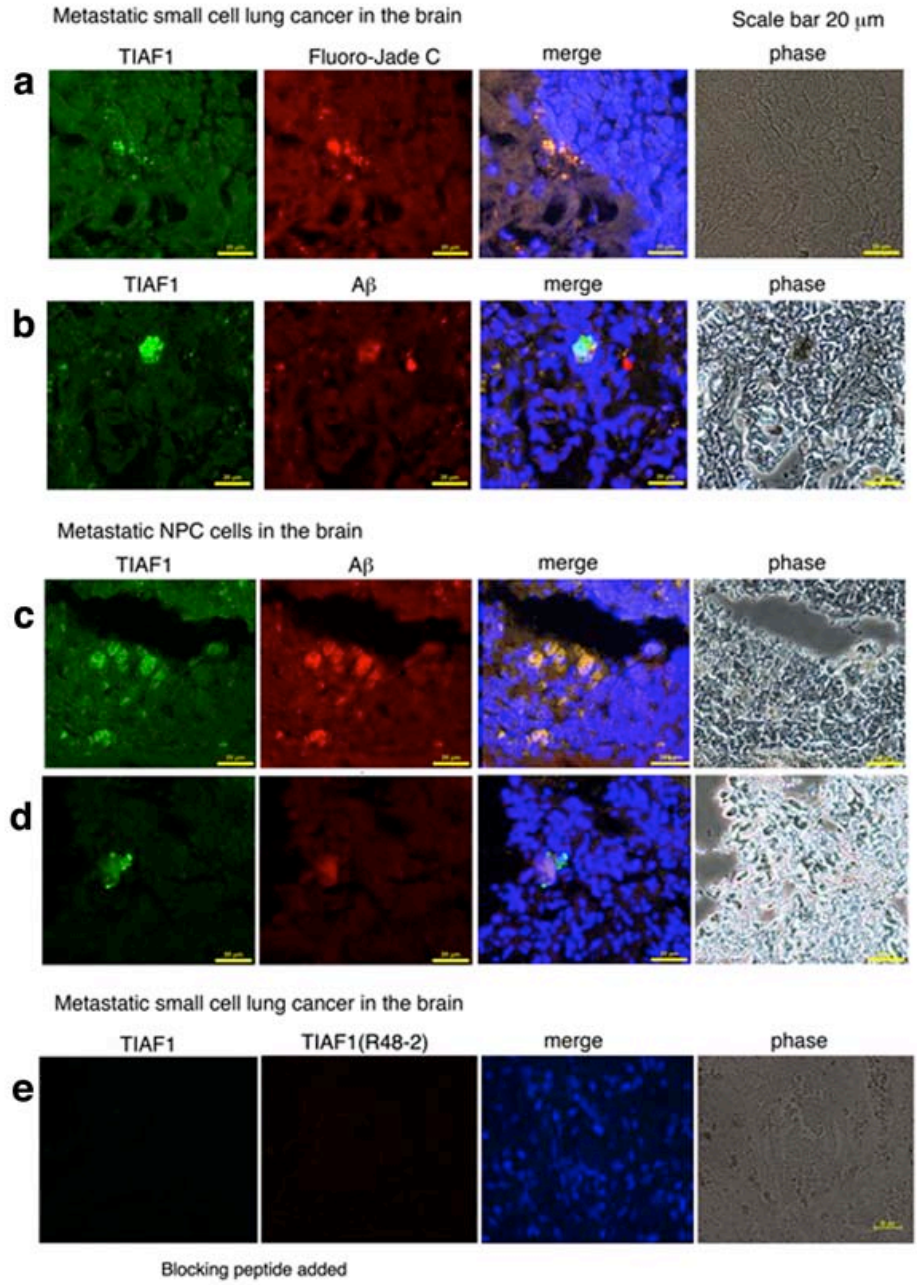


*Fig. S7*

**Figure S8. TIAF1 aggregation in the brain metastatic cancer (from additional specimens)**.

**(a)** TIAF1 aggregates are found around the vicinity between the metastatic small cell lung cancer (lower left; see the dense nuclear stain) and the brain tissue (top right). Degenerating neural cells were stained with Fluoro-Jade C Red. Nuclei were stained with DAPI. Scale bar, 20 μm; 400x magnification. **(b)** Similarly, TIAF1 aggregates are found in a metastatic colon cancer in the brain. Scale bar, 20 μm; 400x magnification. **(c,d)** Presence of TIAF1 and Aβ aggregates is shown in the metastatic lung adenocarcinoma and nasopharngeal carcinoma (NPC) in the brain. TIAF1, green; Aβ, red; nuclei, blue. Scale bar, 20 μm; 400x magnification. (**e**) A representative negative control staining using blocking R48-2 peptide is shown. Scale bar, 20 μm; 400x magnification.

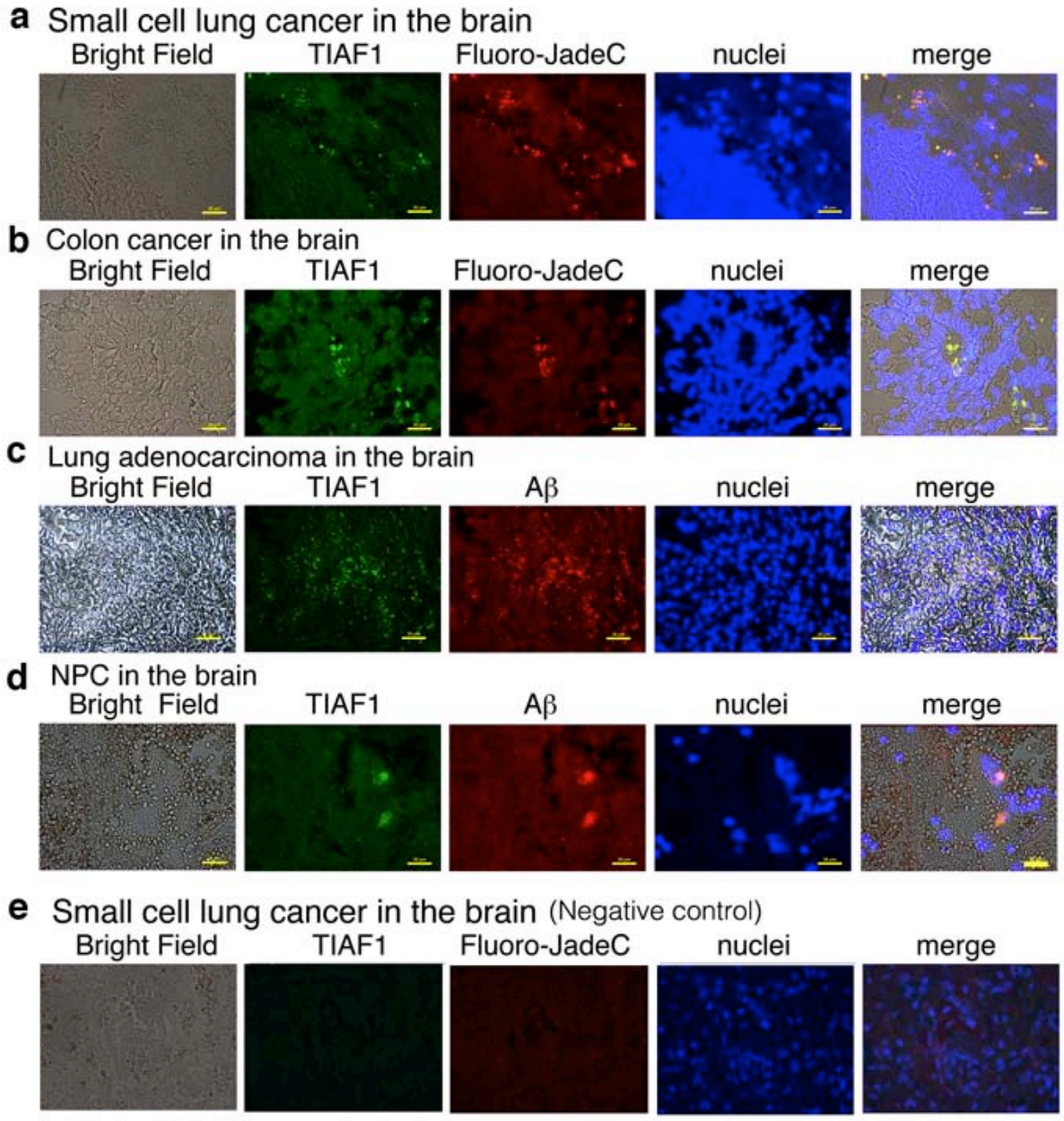


***Fig. S8***

**Figure S9. Presence of TIAF1 and Smad4 fibrous aggregates in prostate cancer.**

Representative pictures are shown, which were taken surrounding the peritumor areas. TIAF1 fibrils are digitally magnified approximately 20-fold from the TIAF1 picture (lower left). The "non-immune serum" control is shown in Figure 1c, and blocking peptide controls in Figure S4.

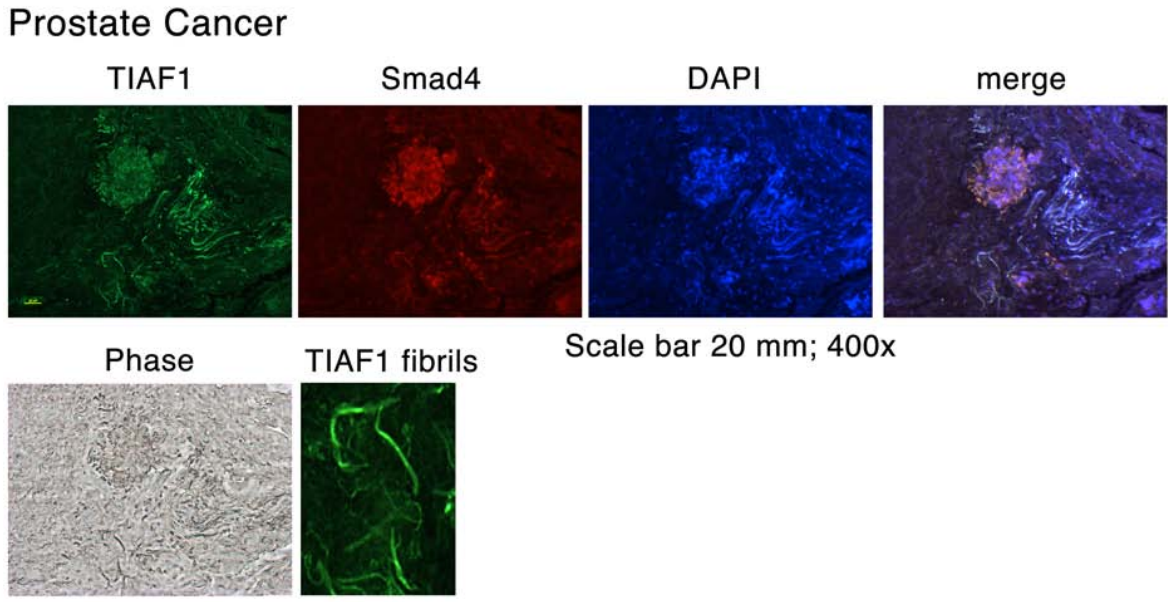


***Fig. S9***

**Figure S10. TIAF1 self-association induces expression of Smad4.**

MCF7 cells were transiently transfected with ECFP-TIAF1 and EYFP-TIAF1 by liposome. The expressed proteins underwent self-binding, and further induced Smad4 expression (see Figure 5a). The induced Smad4 (red) colocalizes with ECFP-TIAF1 (cyan) and EYFP-TIAF1 (yellow) in the cytoplasm and the spiny protrusion (400x magnification). A negative control using the R48-2 blocking peptide is shown in the Figure 5c.

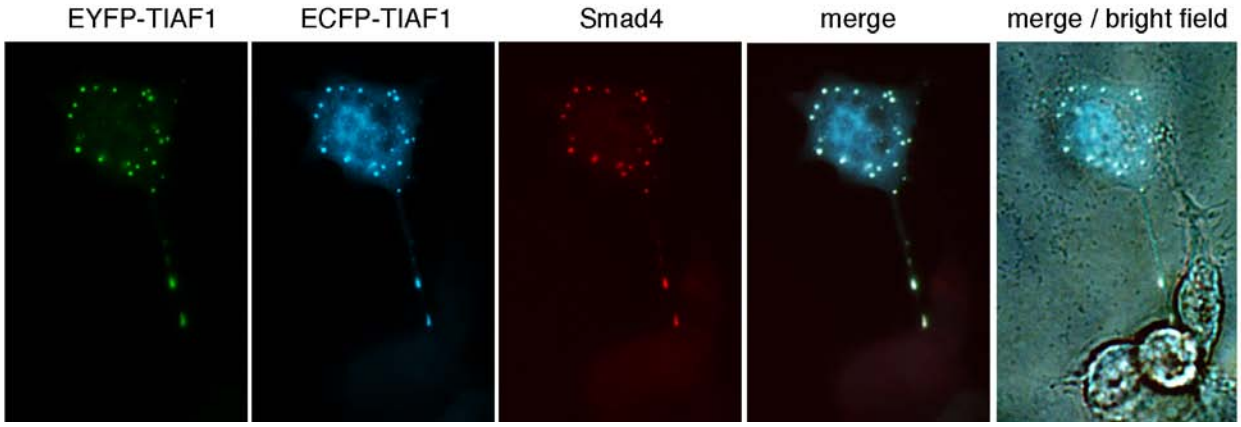


***Fig. S10***

**Figure S11. TIAF1, WOX1, and p53 block the migration of breast cancer cells. (a)** In agreement with the observations using L929 cells (Figure 7c), breast MDA-MB-231 cells were responsive to the inhibitory effect of transiently overexpressed p53, WOX1, and/or TIAF1 in combinations, on cell migration (mean ± standard deviation; n=3; Student's *t* test). The number on the top of each bar is the *p* value from controls versus each indicated protein. The effect of WW or SRD domain of WOX1 was also tested. (**b**) WOX1 and p53 alone inhibited the migration of MCF7 cells. The effect was reduced when p53, WOX1, and TIAF1 were in combinations (mean ± standard deviation; n=3; Student's *t* test).

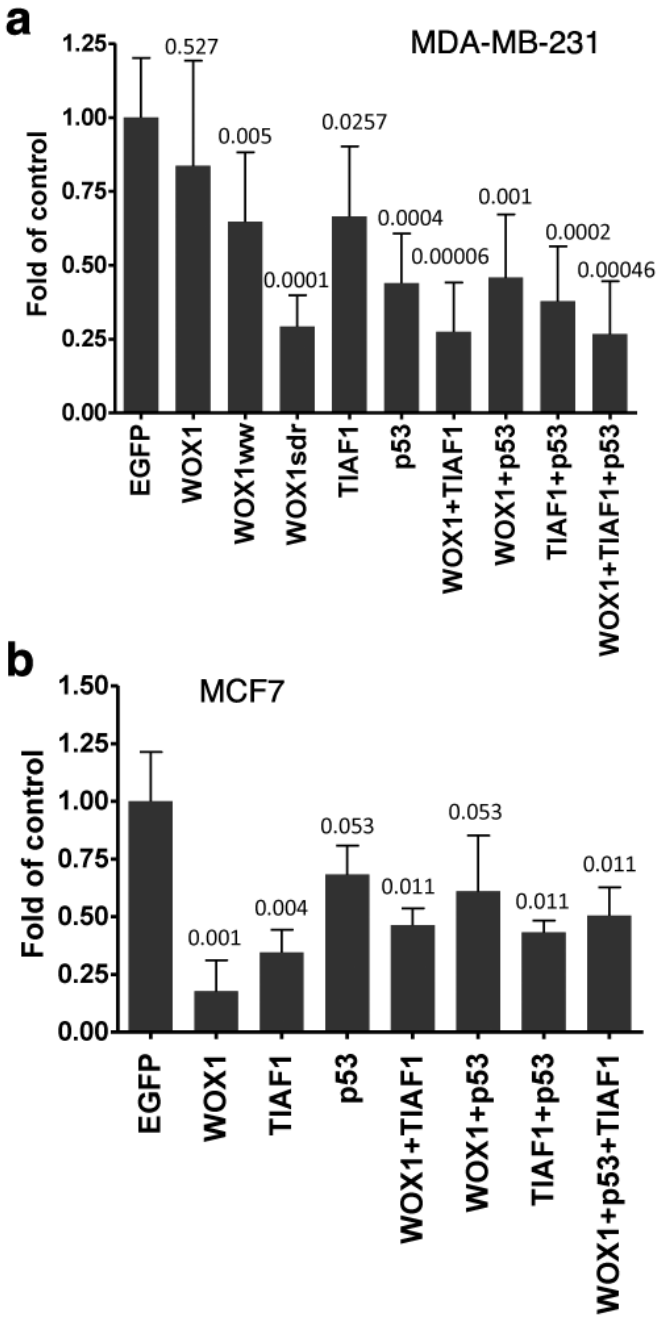


***Fig. S11***